
Article:
Wang, W., Huang, J., Ding, H. orcid.org/0000-0003-0094-8646 et al. (4 more authors) (2024) Initiation and evolution of wheel polygonal wear: influence of wheel-rail hardness ratios. Wear, 540-541. 205255. ISSN 0043-1648

https://doi.org/10.1016/j.wear.2024.205255

Initiation and evolution of wheel polygon wear: Influence of wheel-rail hardness ratios

Wenjian Wang[a], Jinwei Huang[a], Haohao Ding[a,*], Zefeng Wen[a], Xiaolu Cui[b], Roger Lewis[c], Qiyue Liu[a]

a. State Key Laboratory of Rail Transit Vehicle System, Southwest Jiaotong University, Chengdu 610031, China

b. School of Mechatronics and Vehicle Engineering, Chongqing Jiaotong University, Chongqing, China

c. Department of Mechanical Engineering, The University of Sheffield, Mappin Street, Sheffield, S1 3JD, UK

Abstract: Railway wheel polygon is a type of uneven wear of material which worsens the running stability of trains. As a significant factor influencing the wear, wheel-rail hardness matching (i.e., the hardness ratio H_W/H_R) might affect the formation of wheel polygon. Thus, rolling-sliding wear tests were conducted using three wheel steels matching two rail steels to explore the influence of H_W/H_R (ranging from 0.649 to 1.263) on the initiation and evolution of wheel polygon wear. The results show that when matching the softer rail, the wheel was less likely to become polygonal with an increase in H_W/H_R. When matching the harder rail, the wheel presented earlier polygon initiation under a moderate H_W/H_R of 0.792. The largest H_W/H_R of 1.263 presented the best anti-polygon condition for wheel material. The wear mechanism of polygonal wheel was dominated by abrasive, fatigue and oxidative wear at the crest and fatigue wear at the trough.

Keywords: Wheel polygon wear; Hardness ratio; Microstructural deformation; Damage

1. Introduction

Wear is inevitable during the service of the wheel-rail system of a railway [1-3]. The wheel polygon is one of the common wear forms, which deteriorates the dynamic response of the vehicle-track system and accelerates the fatigue failure of its core components [4-10]. In recent years, studies have been carried out from the aspect of vehicle-track dynamics to explore the formation process and mechanism of wheel polygon wear under various operating conditions. However, neither uniform conclusions nor consensus have been reached so far. Therefore, the initiation and development mechanism of the wheel polygon wear are still a pending problem in

*Corresponding author. Tel: +86-28-87634304.
E-mail address: haohao.ding@swjtu.edu.cn (H.H. Ding).

the railway engineering field [11-14].

It is worth pointing out that, as a type of wear, the wheel polygon is closely related to the wheel and rail material properties. Some scholars believe that the formation of the wheel polygon is highly affected by the material mechanical properties and the manufacturing process [15], such as the roughness and the hardness of wheel tread, the uneven distribution of material microstructure and the wheel eccentricity. Nielsen et al. [16,17] proposed that the roughness at certain wavelengths of the worn wheel tread increased with the running distance, which could enlarge the wheel-rail contact force and make the irregular wear gradually develop into periodic wear. Song et al. [18] found that compared with wheels without polygon wear, the hardness of the wheels with polygon wear was smaller. Therefore, the wheel with lower hardness was more likely to become polygonal and that adjustment of the wheel hardness could be an essential method to inhibit the initiation and the development of wheel polygons. Furthermore, Shen et al. [19] proposed a rolling strengthening method considering the residual stress and improving the hardness on the wheel surface, which could be used to reduce polygon wear.

In reality, wheels and rails with various hardness are used. However, the influence of hardness ratios of wheel and rail materials on the formation of wheel polygon wear is not clear. Therefore, rolling-sliding tests were carried out under various wheel-rail hardness ratios (H_w/H_r) to explore the initiation and evolution of wheel polygon wear. In particular, for the real time detection of the wheel polygon wear development, the wear morphology of the wheel sample is observed and the vibration of wheel-rail samples is detected without stopping the test. Then, influences of the H_w/H_r on the wheel polygon wear are discussed. Furthermore, the initiation and evolution mechanism of wheel polygon wear are explored by means of various macroscopic and microscopic examinations.

2. Experimental details

2.1 Experimental machine and samples

Tests were conducted on a rolling-sliding wear testing apparatus [20], as shown in Fig. 1a. The servo motor drives the lower roller (wheel sample) and upper roller (rail sample). The difference of rotational speeds between wheel and rail rollers is obtained through adjusting the gear pairs. The vertical force is applied by a spring. A vibration sensor is installed on the bearing pedestal of the lower shaft to collect the vibration signal.

The sampling positions and dimensions of the wheel and rail rollers are shown in Fig. 1b. They are taken from the wheel tread and the railhead and machined into the desired size with a surface roughness of 0.2 μm. The diameter and thickness of the roller sample are 40 mm and 10 mm, respectively. Furthermore, to form an elliptic wheel/rail contact, the edge of wheel roller was machined into an arc shape with a radius of 14 mm in the axial direction. Besides, the arc shape of wheel roller is beneficial for observing the wave shape of wear scar due to the polygon wear by using a high-speed camera (Revealer, China).

To clarify the influence of H_W/H_R on the formation and evolution of wheel polygon wear, six groups of tests were performed using three types of wheel steels (ER8C, B-class and C-class) matching two types of rail steels (U71Mn and PG5). The chemical compositions and the hardness of materials are listed in Table 1 [21]. And the wheel/rail hardness ratios (H_W/H_R) of six groups are listed in Table 2.

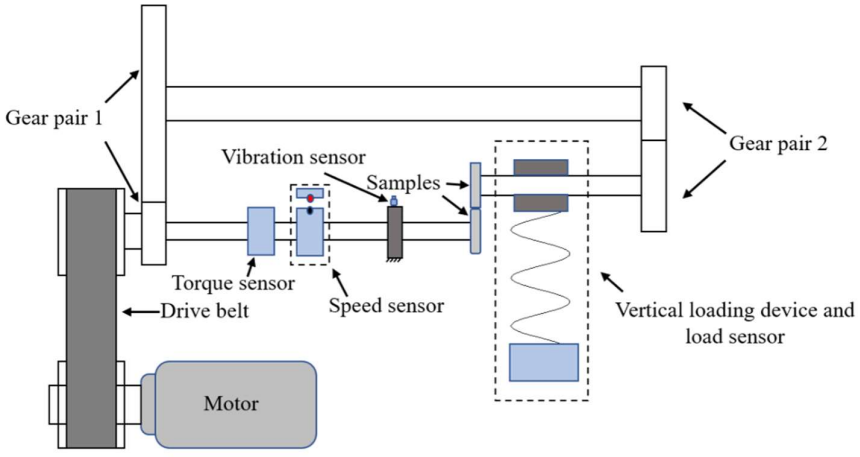

(a)

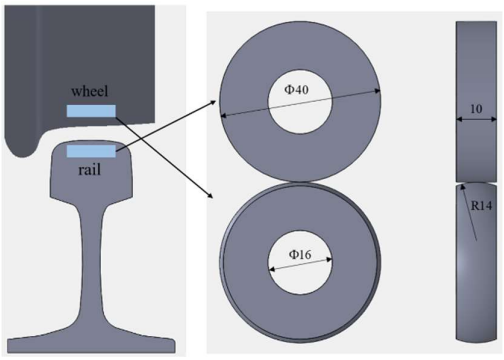

(b)

Fig. 1. Schematic diagrams: (a) testing machine; (b) wheel-rail roller samples

Table 1 Chemical compositions and hardness of wheel and rail materials.

Component	Grade	Chemical composition (wt%)					Hardness/$HV_{0.5}$
		C	Si	Mn	P	S	
Wheel	ER8C	0.54~0.56	0.90~1.10	0.90~1.10	≤0.01	≤0.010	279±4
	B-class	0.57~0.67	0.15~1.00	0.60~0.90	0.03	0.005~0.040	327±8
	C-class	0.67~0.77	0.15~1.00	0.60~0.90	0.03	0.005~0.040	360±6
Rail	U71Mn	0.65~0.76	0.15~0.58	0.70~1.20	≤0.03	≤0.025	289±6
	PG5	0.80~1.00	0.10~0.80	0.40~1.30	≤0.02	≤0.020	424±9

Table 2 Different wheel-rail hardness ratios.

Rail \ Wheel	C-class	B-class	ER8C
U71Mn	1.263	1.198	0.976
PG5	0.853	0.792	0.649

2.2 Experimental procedure

The wheel was run under a traction condition in the test owing to fact that serious polygon wear is mainly concentrated on the traction wheels [22]. The rotational speeds of wheel and rail rollers were 212 r/min and 202.354 r/min, respectively to realize a positive wheel/rail slip ratio of 4.55%. A vertical force of 350 N between the wheel and rail rollers was applied to simulate a maximum contact stress of 1881 MPa which is common in the field [23]. Furthermore, the

number of cycles in the tests was set at 150,000 cycles.

Before testing, the rollers were cleaned for 20 minutes using anhydrous ethanol in ultrasonic cleaning instrument to ensure that the roller surfaces were free from oil pollution, oxide and other contaminants. A Vickers microhardness tester (MVK-H21, Japan) was used to measure the surface and subsurface hardness of the rollers. The formation of wheel polygons induces vibrations in the wheel-rail system. Therefore, a UXI-50016 dynamic testing system was used to monitor the vibration signal during the tests. The formation process of polygon wear was also qualitatively observed using a high-speed camera (Revealer, China). After testing, the polygon characteristic was measured and analyzed using a wheel out-of-round laser measuring instrument. The macroscopic and microscopic observations of polygonal wheel material were performed using the optical microscope (KEYENCE VHX-6000, Japan) and scanning electronic microscope (SEM) (Phenom Pro, the Netherlands).

3. Results

3.1. Polygonal wear behavior

The out-of-roundness of wheel rollers after the test (150,000 cycles) is shown in Fig. 2. In each subgraph, the polygonal profile and the order analysis result calculated through a Hilbert-Huang transform method [24,25] are given on the left and right sides, respectively. Fig. 3 shows the amplitude of the wheel polygon, i.e., the difference between the heights at the crest and trough.

It can be seen that when rolling against the softer rail (U71Mn rail), the hardest wheel (C-class wheel, H_W/H_R: 1.263) presents no polygon wear. The circumferential profile has a regular circle shape and the polygon amplitude is 0. As H_W/H_R decreases to 1.198 (B-class wheel) and to 0.976 (ER8C wheel), the circumferential profiles change periodically and the polygon amplitude has an increasing trend. Obvious 21st order out-of-round forms on both B-class and ER8C wheels. When matching with the harder rail (PG5 rail), the hardest wheel (C-class wheel, H_W/H_R: 0.853) presents a very slight polygon wear with 21st order. As the H_W/H_R decreases to

0.792 (B-class wheel) and to 0.649 (ER8C wheel), obvious polygon wear with 20th order is generated and the polygon amplitudes increase.

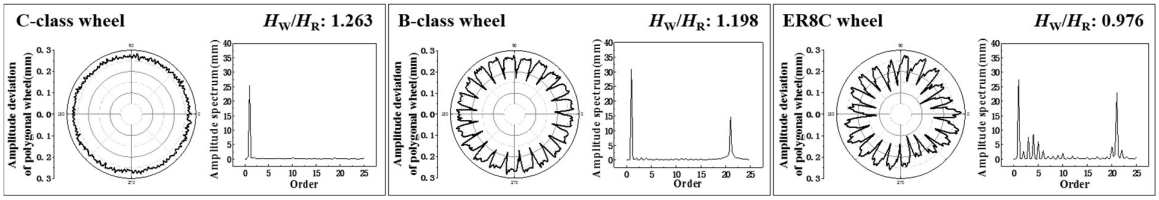

(a)

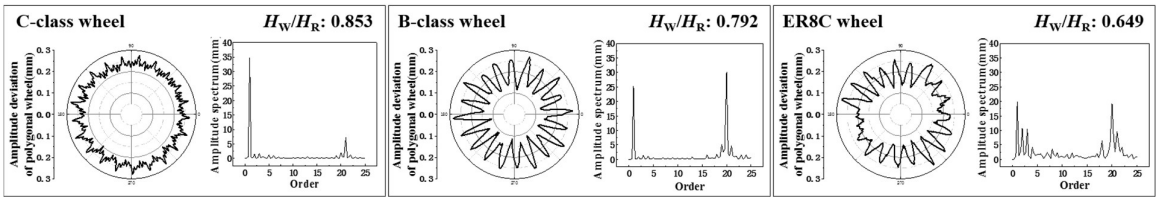

(b)

Fig. 2. Polygonal profiles and orders of wheels when rolling against (a) U71Mn rail and (b) PG5 rail.

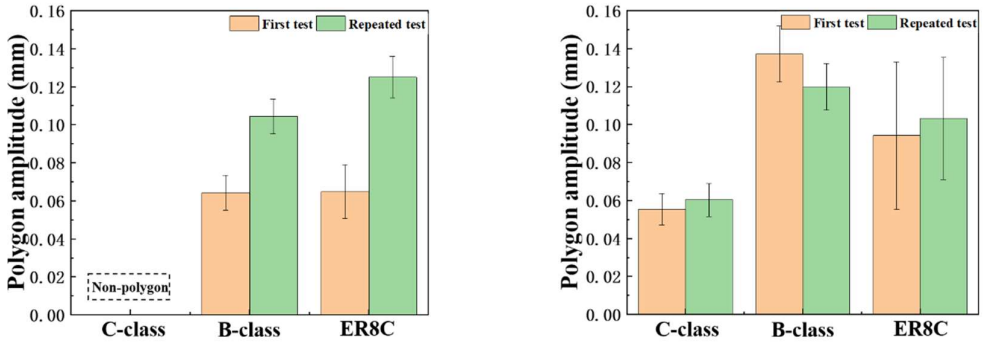

(a) (b)

Fig. 3. Amplitudes of wheel polygons when rolling against (a) U71Mn rail and (b) PG5 rail.

In order to analyse the evolution process of wheel polygon wear, the topography of wheel roller was observed via a high-speed camera and the variation of wheel roller was detected using a vibration sensor. When the polygon wear is formed, an excitation frequency could be detected. So, the formation and development process of wheel polygon could be labeled by monitoring the vibration of wheel-rail rollers in addition to the observation of the high-speed camera photos. The vibration is correlated with the polygon order and the rotational speed. In this study, Fourier analysis was used to describe the polygon wear of wheel roller with different orders [26].

Wavelength could be defined as follows:

$$\lambda_{n=}2\pi r/n_{oor,}\ n_{oor=}1,2,3,\ldots,n, \tag{1}$$

where, n_{oor} is polygon order, r is the wheel radius.

When the linear speed is v (m/s), the excitation frequency could be calculated through equation (2):

$$f_{oor}=v/\lambda_n \tag{2}$$

The relationship between the linear speed and rotational speed n (r/s) is:@

$$v=2\pi r\cdot n \tag{3}$$

So, the relationship between the excitation frequency (f_{oor}) and the wheel polygon order (n_{oor}) can be obtained as follows:

$$f_{oor}=n_{oor}\cdot n \tag{4}$$

Figs. 4 and 5 show the photos and the vibration signal with the increase in the number of cycles, respectively. When rolling against the softer rail (U71Mn rail), when the hardest wheel (C-class wheel) formed no polygon wear during the test, the width of the wear scar increased with the number of cycles, and the edge of the worn scar was smooth. Also, no vibration was excited. For the softer wheel (B-class wheel), before 120, 000 cycles, the wear scar is even, and no vibration was excited. After 120, 000 cycles, uneven wear occured and a vibration frequency of 74 Hz was excited. So, the initiation life of the polygon wear is 120, 000 cycles. Meanwhile, according to equation (4), the frequency of 74 Hz is the characteristic frequency of 21st order wheel polygons, which is consistent with the circumferential profile (Fig. 2). For the softest wheel (ER8C wheel), polygon wear was formed after 90,000 cycles. When rolling against the harder rail (PG5 rail), very slight polygon wear was observed on the hardest C-class wheel at 150,000 cycles. For softer (B-class) and the softest (ER8C) wheels, obvious polygon wear forms rapidly, at around 30,000 cycles and 60, 000 cycles respectively.

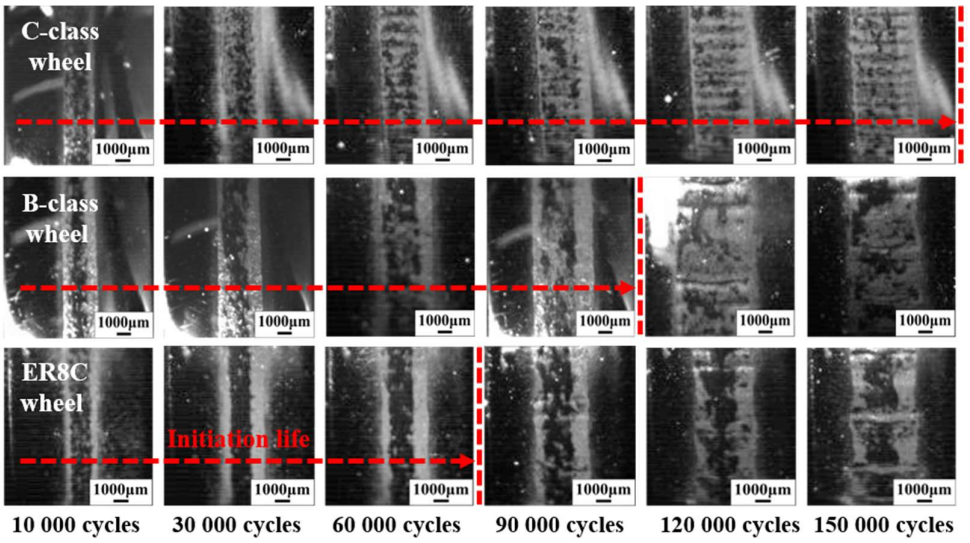

(a)

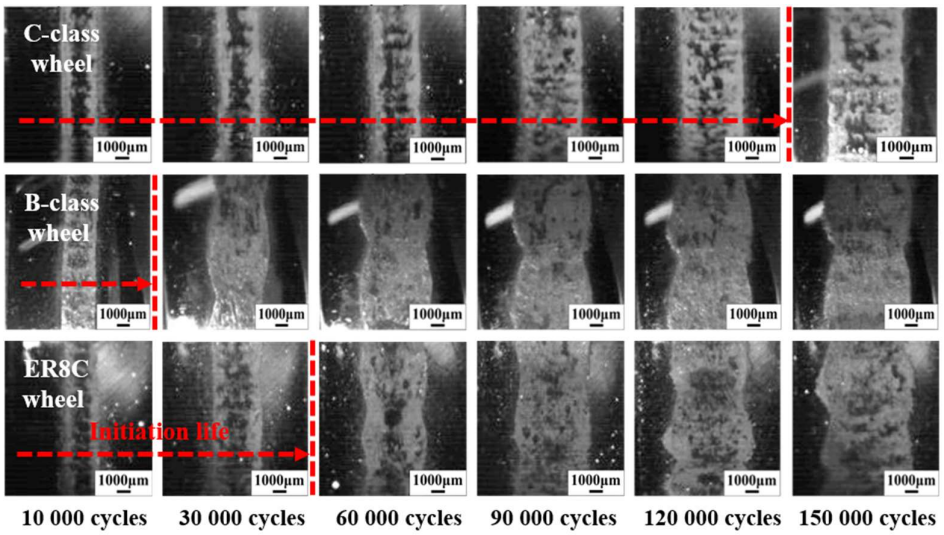

(b)

Fig. 4. Wheel wear scar with cycle number when rolling against (a) U71Mn rail and (b) PG5 rail.

It has been shown that, both the wheel and rail hardness influence the formation of wheel polygon wear. Concerning the influence of wheel hardness, polygon wear is difficult to form on the hardest wheel (C-class wheel), i.e., no polygon wear was generated during the test (150, 000 cycles) when rolling against the softer rail (U71Mn), and only slight polygon wear was generated at around 150, 000 cycles when run against the harder rail (PG5). Meanwhile, the polygon amplitude is small. For the softer wheels (B-class and ER8C wheels), polygon wear forms more

easily, i.e., initiation lives (the number of cycles when polygon wear initiate on the wheel) are shorter and the polygon amplitudes are larger. Concerning the influence of rail hardness, when rolling against the harder rail (PG5 rail), the wheel polygon wear forms more easily with smaller initiation lives and larger polygon amplitudes. Above all, it can be concluded that the best anti-polygon wear occurs on the hardest wheel (C-class wheel) rolling against the softer rail (U71Mn).

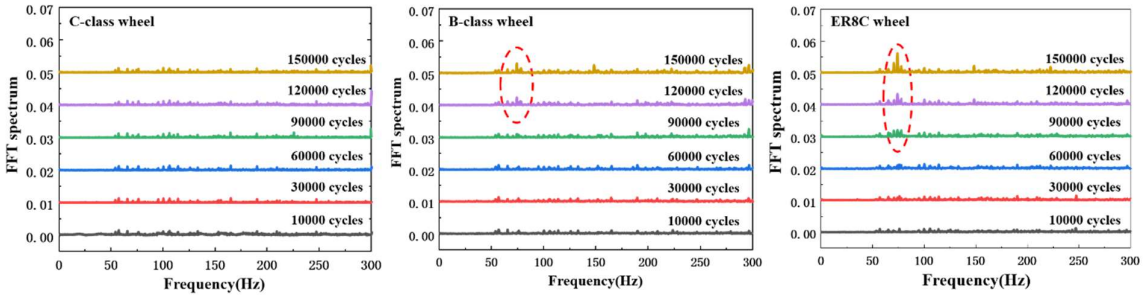

(a)

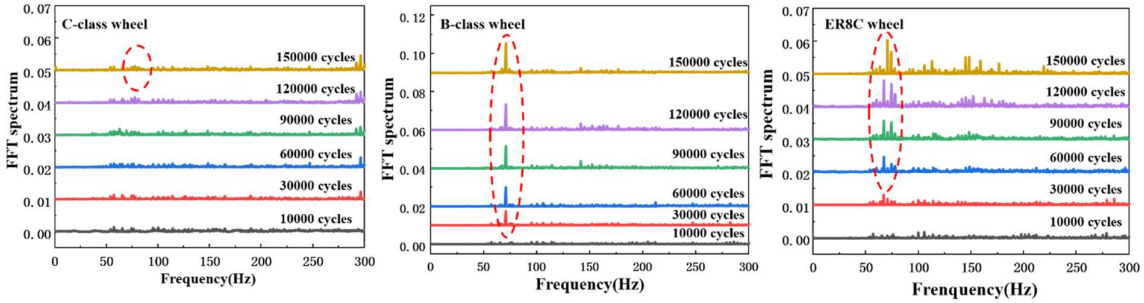

(b)

Fig. 5. Frequency variation of wheel with cycle number when rolling against (a) U71Mn rail and (b) PG5 rail.

3.2. Plastic deformation of material

It is observed in Fig. 6 that obvious plastic deformation layers are formed after the test. The original coaxial coarse grains are elongated along the rolling-sliding direction and the microstructure near the outermost surface is almost parallel to the worn surface. For the wheel without polygon (C-class wheel vs. U71Mn rail), the thickness of plastic deformation layer is uniformly distributed along the rolling-sliding direction, and the thickness is in the range of 40-60 μm. For the B-class and ER8C wheel rollers (with polygon), it is clear that the thickness of

plastic deformation layer is unevenly distributed. The plastic deformation layer at the crest is thicker than that at the trough.

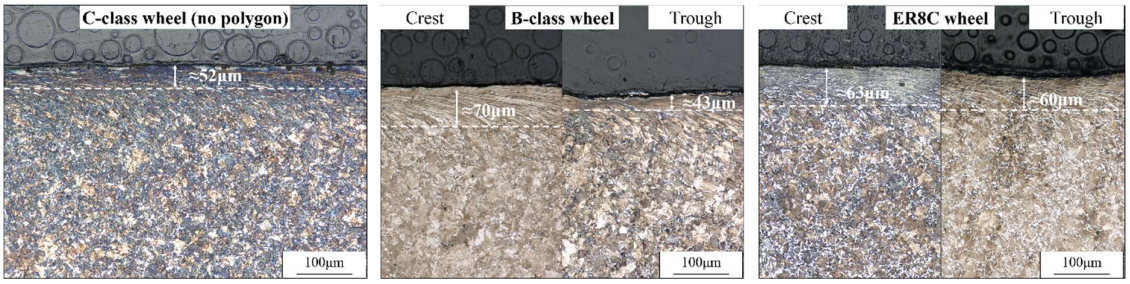

(a)

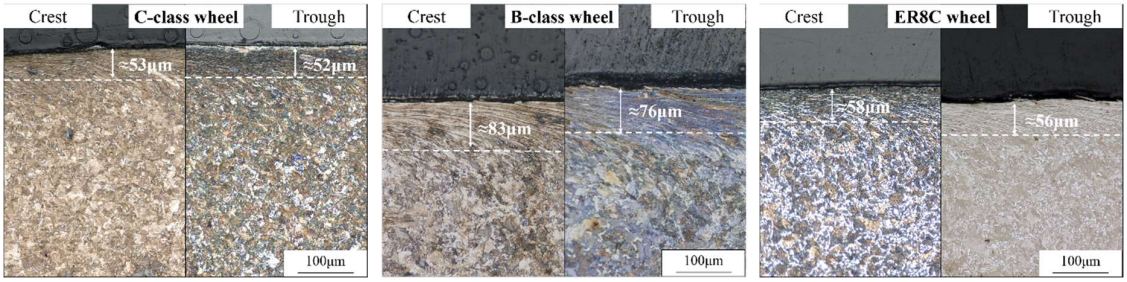

(b)

Fig. 6. Plastic deformation of wheel when rolling against (a) U71Mn rail and (b) PG5 rail.

The hardness was also measured on the cross sections of wheel rollers at different depths: 20, 50, 80, 110, 140 and 170 μm. Fig. 7a shows the subsurface hardness distribution of the C-class wheel (without polygon). It is obvious that the highest hardness appears at the outmost surface. With an increase in the depth, the hardness decreases. Furthermore, the hardness values are similar at the same depth. It is observed in Fig. 7b that the subsurface hardness of the polygonal wheel varies periodically in the rolling-sliding direction. Compared with the surface profile, it can be found that the change in the trend of hardness is opposite to that of the surface profile, i.e., the hardness is lower at the crest region, but higher at the trough region. Furthermore, the opposite relationship is obtained between the hardness and the plastic deformation layer thickness, i.e., the higher hardness and thinner plastic deformation layer occur at the trough. The reason might be that the compacting action at the trough between the wheel and rail increased the working hardening, and then the plastic flow of the hardened material is lighted.

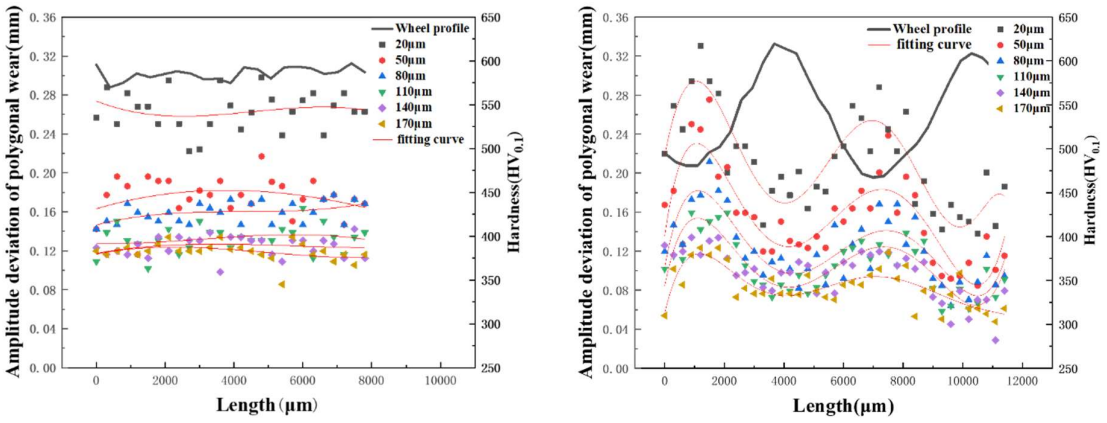

(a) (b)

Fig. 7. Hardness distribution: (a) wheel without polygon (C-class wheel vs. U71Mn rail); (b) polygonal wheel (ER8C wheel vs. PG5 rail).

3.3. Damage behavior

Fig. 8 shows the damage morphologies of the wheel roller without polygon (i.e., C-class wheel vs. U71Mn rail). It can be seen that a third layer (gray in the OM and dark in the SEM) is formed on the surface. This layer is an oxidation layer which might be derived from the wear debris [27]. From the cross section, the microstructure of wheel material deforms along the tangential force during the rolling-sliding contact. The rolling contact fatigue (RCF) crack generates and propagates in a small angle mainly along the material plastic deformation direction (Fig. 8c). Meanwhile, the branch cracks are also generated.

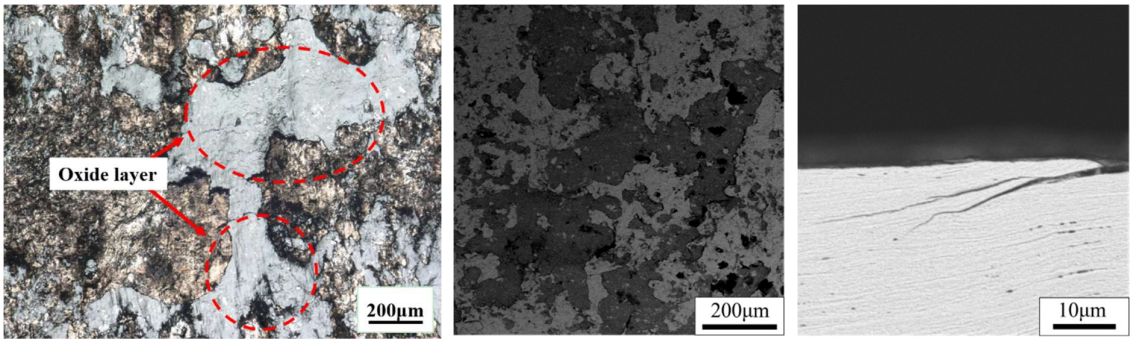

(a) (b) (c)

Fig. 8. Damage morphologies of a wheel without polygon (C-class wheel vs. U71Mn rail): (a) OM of surface; (b) SEM of surface; (c) SEM subsurface image of RCF cracks.

Figs. 9 and 10 show the damage morphologies of the crest and trough of the polygonal wheel (i.e., ER8C wheel vs. PG5 rail), respectively. It is clear that the crest surface is dominated by ploughing and oxide layers. The ploughing direction is nearly parallel to the rolling-sliding direction. From the cross section, the RCF crack characteristic is similar to that of the wheel without polygon (Fig. 8c). The crack propagates along the material plastic flow direction. Besides, under the repeated contact action, the interlayer in the space of the crack is broken and the material above the crack is fractured. Thus, abrasive wear, oxidative wear and fatigue wear are predominant at the crest. It is clear from Fig. 10 that the damage morphology at the trough is different compared to that at the crest. On the surface, only a few oxide spots exist. On the cross section, RCF cracks are short and tend to branch. Furthermore, subsurface cracks are formed, which could connect with adjacent cracks to form the spalling. Thus, the damage form at the trough is dominated by fatigue wear.

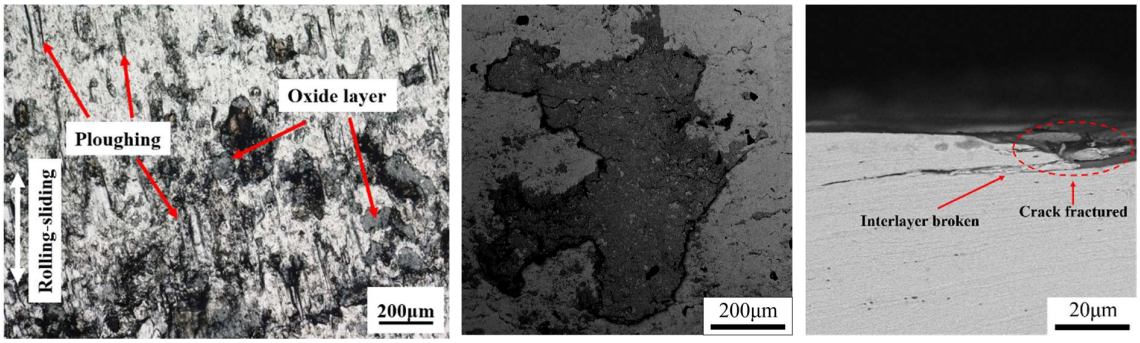

(a) (b) (c)

Fig. 9. Damage morphologies of the crest of a polygonal wheel (ER8C wheel vs. PG5 rail): (a) OM of surface; (b) SEM of surface; (c) SEM subsurface image of RCF cracks.

Statistical results of crack lengths, depths and angles of wheel rollers under various hardness ratios are given in Fig. 11. Each point in the figure represent one crack. The average crack length, depth and angle of the wheel without polygon (C-class wheel vs. U71Mn rail) are in the ranges of 13.9~48.7 μm, 3.5~10.4 μm and 9.3°~19.6°, respectively. For polygonal wheels, the crack length and depth at the crest are slightly larger than those at the trough. The difference is more

obvious on the wheels when rolling against the hard rail (PG5 rail) during which the polygon wear of wheel is more severe. In terms of the crack angle, there is no obvious difference between the crest and the trough for wheels rolling against the soft rail (U71Mn rail) and for C-class wheel against the PG5 rail. For the B-class and ER8C wheels against PG5 rail, the RCF crack angle is larger on the crest than on the trough.

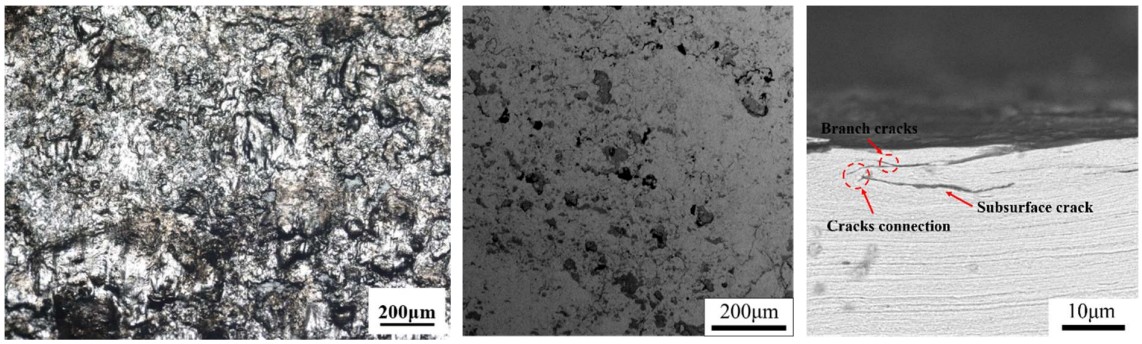

(a) (b) (c)

Fig. 10. Damage morphologies of the trough of a polygonal wheel (ER8C wheel vs. PG5 rail): (a) OM of surface; (b) SEM of surface; (c) SEM subsurface image of RCF cracks.

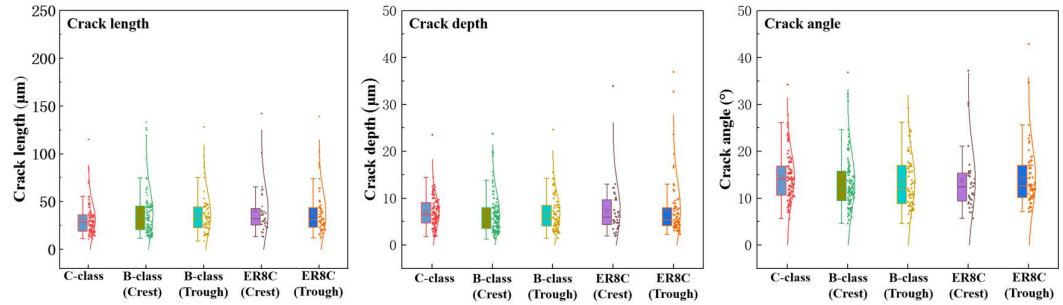

(a)

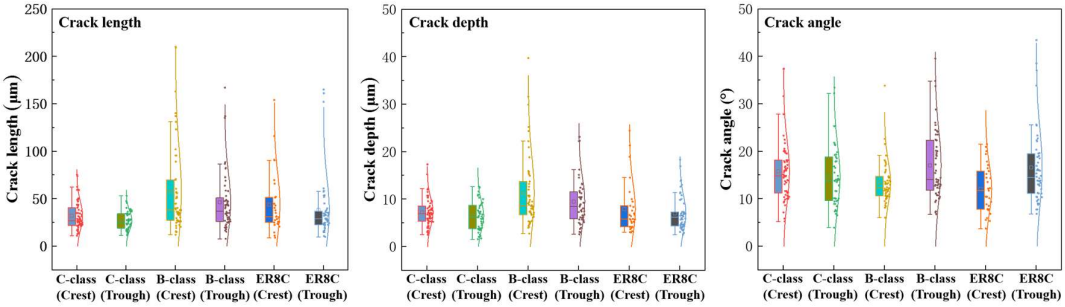

(b)

Fig. 11. Crack length, depth and angle of wheels when rolling against (a) U71Mn rail and (b) PG5 rail.

4. Discussion

It is novel to explore the initiation and evolution mechanism of wheel polygon from the aspect of the material properties. A hypothesis on the initiation mechanism of wheel polygon can be proposed, as shown in Fig. 12. During the rolling-sliding contacts, the wheel surface is subjected to compressive and tangential stresses, which deforms the microstructure of wheel material (pearlite) severely. With the increase in the number of cycles, due to the mechanical vibration of the test apparatus, which can be regarded as the vibration of the vehicle-track system in the field, local areas of wheel surface suffer from additional impact compressive stresses. Therefore, the plastic deformation and surface hardness of the impacted area increase gradually due to the repeated external compressive stress. As a result, the wheel surface material begins to form uneven hardening [28]. Wheel circumferential uneven hardness will lead to uneven wear and the formation of the initial out-of-round wheel [29]. This provides the condition for the vertical self-excited vibration of wheel-rail system, resulting in the initiation of wheel polygons [30-32]. When the polygon excitation frequency is coupled with the natural frequency of the wheel-rail system, resonance would be generated and the formation of wheel polygon is intensified [33].

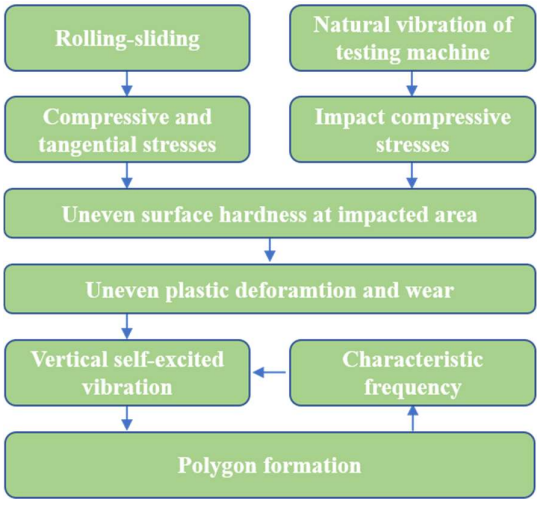

Fig. 12. Hypothesis on the wheel polygon formation mechanism.

It is found from Fig. 13 that the formation of wheel polygon is closely related to the H_W/H_R.

As a whole (considering three types of wheels and two types of rails), with anincrease in the H_W/H_R, the polygon was formed more easily, i.e., the polygon initiation life increased (Fig. 13a) and the amplitude of the polygon decreased (Fig. 13b). This is because the polygon wear is a type of wear forms. Material with stronger ability to resist wear needed more cycles for the above initial out-of-round conditions to occur, and would generate a harder wheel polygon. With the increase in H_W/H_R, the wear loss of the wheel roller was decreased (Fig. 13c), which means that the wear resistance became higher [34]. Therefore, when matching with the U71Mn rail (softer rail), there was no polygon on the C-class wheel under the largest H_W/H_R of 1.263. While, the other wheels (B-class and ER8C) generated polygon wear because of the decreased H_W/H_R.

When rolling against the PG5 rail (harder rail), the ER8C wheel which had the smallest H_W/H_R (0.649) generated the polygon later than the B-class wheel (H_W/H_R: 0.792). This is because the chemical compositions of wheel materials also affected its wear performance. Besides, increasing the content of Si and Mn in wheel material can improve its wear resistance [35]. Thus, the wear resistance of ER8C wheel (with larger Si and Mn contents, Table 1) might be stronger than the B-class wheel (Fig. 13c). Among all the studied wheel-rail matches, the hardest wheel (C-class wheel) rolling-sliding against the softer rail (U71Mn rail) presented the best anti-polygon combination.

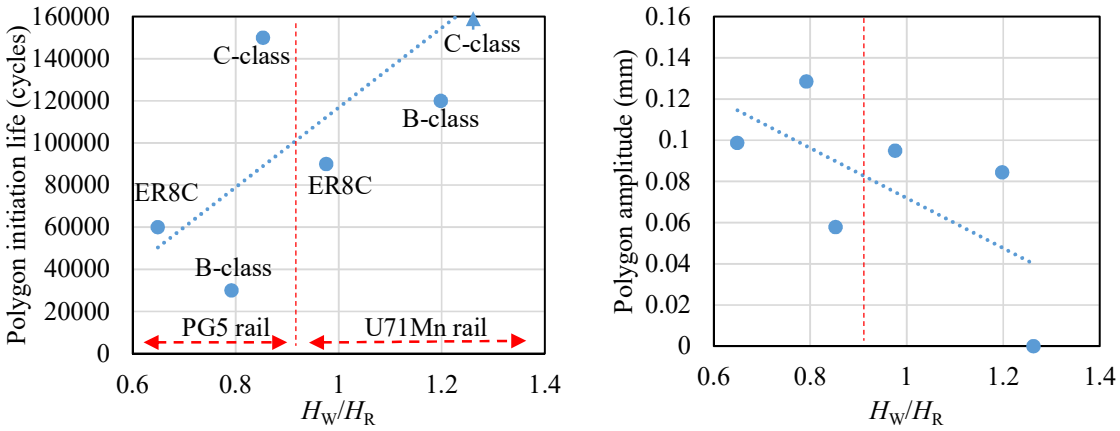

(a) (b)

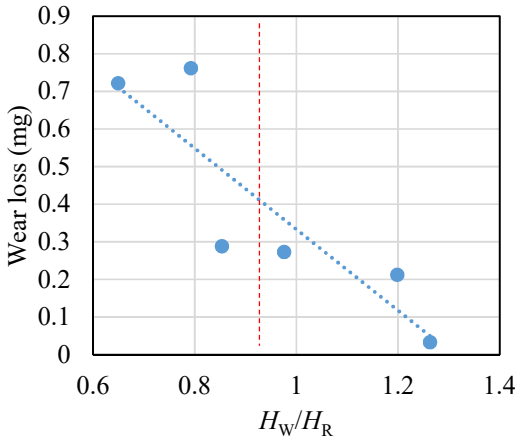

(c)

Fig. 13. (a) Polygon initiation life, (b) average polygon amplitude after test and (c) wear loss as a function of wheel-rail hardness ratio.

5. Conclusions

(1) Both the hardness of wheel and rail influenced the formation of wheel polygon wear. With an increase in the wheel hardness, it was more difficult for polygons to form. And the polygon wear initiation life increased while the polygon amplitude decreased. With an increase in the rail hardness, the wheel polygon wear was formed more easily with smaller initiation lives and larger polygon amplitudes. The best anti-polygon wear resistance occurred on the wheel under the largest H_W/H_R condition.

(2) For the wheel without polygon, the wear mechanism is dominated by oxide wear and fatigue wear. The hardness and plastic deformation of the microstructure was distributed evenly in the circumferential direction. The material hardening increased when approaching the surface in the cross section. RCF cracks mainly propagated along the plastic deformation direction.

(3) For the polygonal wheel, the wear mechanism was dominated by abrasive wear, fatigue wear and oxidative wear at the crest, and by fatigue wear at the trough. RCF cracks at the crest were longer and deeper than those at the trough. The thickness of plastic deformation layer and the hardness were periodically distributed in the circumferential direction. Comparing with the crest, the trough region presented a thinner plastic deformation layer, higher hardness and smaller

RCF cracks.

(4) The formation of wheel polygons was related to the ability to resist wear of wheel material under various H_W/H_Rs. Uneven surface hardening would occur under the external compressive stress, leading to the uneven wear, which provided the condition for the vertical self-excited vibration of wheel-rail interface, resulting in the initiation of wheel polygon. When the polygon excitation frequency was coupled with the natural frequency of wheel-rail interface, the polygon was developed.

Declaration of Competing Interest

The authors declare that they have no known competing financial interests or personal relationships that could have appeared to influence the work reported in this paper.

Acknowledgments

The work was supported by National Natural Science Foundation of China (Nos. U21A20167, 51975489, 52275176).

References

[1]Hu Y, Zhou L, Ding HH, Lewis R, Liu QY, Guo J, Wang WJ. Microstructure evolution of railway pearlitic wheel steels under rolling-sliding contact loading. Tribology International 154 (2021) 106685.

[2]Wang YP, Ding HH, Zou Q, Xiao F, Zhang XF, Wang WJ, Guo J, Liu QY. Research progress on rolling contact fatigue of railway wheel treads. Surface Technology 49(5) (2020)120-128.

[3]Zhang SY, Spiryagin M, Ding HH, Wu Q, Guo J, Liu QY, Wang WJ, . Rail rolling contact fatigue formation and evolution with surface defects. International journal of fatigue 158 (2022) 106762.

[4]Wu X, Chi M, Gao H. Damage tolerances of a railway axle in the presence of wheel polygonalizations. Engineering Failure Analysis 66 (2016) 44-59.

[5]Wang Z, Mei G, Zhang W, Cheng Y, Zou H, Huang G, Li F. Effects of polygon wear of wheels on the dynamic performance of the gearbox housing of a high-speed train. Proceedings of the Institution of Mechanical Engineers-Part F: Journal of Rail and Rapid Transit 232(6) (2018) 1852-1863.

[6]Wu H, Wu P, Li F, Shi H, Xu K. Fatigue analysis of the gearbox housing in high-speed trains under wheel polygonization using a multibody dynamics algorithm. Engineering Failure Analysis 100 (2019) 351-364.

[7]Chen M, Sun Y, Guo Y, Zhai W. Study on effect of wheel polygon wear on high-speed vehicle-track-subgrade Vertical Interactions. Wear 432-433 (2019) 102914.

[8]Shen X, Lu L, Zeng D. Fatigue failure analysis of high strength bolts used for high-speed railway vehicle braking discs. Engineering Failure Analysis 115 (2020) 104661.

[9]Wang B, Xie S, Jiang C, Song Q, Sun S, Wang X. An investigation into the fatigue failure of metro vehicle bogie frame. Engineering Failure Analysis 118 (2020) 104922.

[10]Peng B, Iwnicki S, Shackleton P, Crosbee D. Comparison of wear models for simulation of railway wheel polygonization. Wear 436-437 (2019) 203010.

[11]Fu B, Stefano B, Luo SH. Study on wheel polygonization of a metro vehicle based on polygon wear simulation. Wear 438-439 (2019) 203071.

[12]Vernersson T. Thermally induced roughness of tread braked railway wheels. Wear 236(1) (1999) 106-116.

[13]Bracciali A, Cascini G. Detection of corrugation and wheelflats of railway wheels using energy and cepstrum analysis of rail acceleration. Proceedings of the Institution of Mechanical Engineers, Part F: Journal of Rail and Rapid Transit 211(2) (1997)109-116.

[14]Feller HG, Walf K. Surface analysis of corrugated rail treads. Wear 144(1-2) (1991) 153-161.

[15]Zhu HY, Hu HT, Yin BC, Wu PB, Zeng J, Xiao Q. Research progress on wheel polygons of rail vehicles. Journal of Traffic and Transportation Engineering 20(1) (2020) 70-77.

[16]Nielsen JCO, Johansson A. Out-of-round railway wheels-a literature survey. Journal of Rail and Rapid Transit 214(2) (2000) 79-91.

[17]Nielsen JCO, Lunden R, Johansson A, Vernersson T. Train-track interaction and mechanisms of irregular wear on wheel and rail surface. Vehicle System Dynamics 40 (2003) 3-54.

[18]Song CY, Shen WL, Li XF, Cui LT. On the influencing factors and inhibiting measures of wheel polygons of high-speed EMUs. China Railway 11(2017) 33-40.

[19]Shen WL, Song CY, Li GD, Li XF, Cui LT. Research for high-speed EMU wheel hardness and polygon-form relationships with solutions. Railway Locomotive and Car 4 (2018)18-23.

[20]Zhang SY, Ding HH, Lin Q, Liu QY, Spiryagin M, Wu Q, Wang WJ, Zhou ZR. Experimental study on wheel-rail rolling contact fatigue damage starting from surface defects under various operational conditions. Tribology International 181 (2023) 108324.

[21]Zhou QY, Liu FS, Zhu M, An T. Research on hardness matching in wheel-rail system. China Railway Science 5 (2006) 35-41.

[22]Zhao XN, Chen GX, Lv JZ, Zhang S, Wu BW, Zhu Q. Study on the mechanism for the wheel polygon wear of high-speed trains in terms of the frictional self-excited vibration theory. Wear 426-427 (2019) 1820-1827.

[23]Wang WJ, Wang H, Wang HY, Guo J, Liu QY, Zhu MH, Jin XS. Sub-scale simulation and measurement of railroad wheel/rail adhesion under dry and wet conditions. Wear 302 (2013)

1461-1467.

[24]Cui DB, Liang SL, Song CY, Deng YG, Du X, Wen ZF. Out of round high-speed wheel and its influence on wheel/rail behavior. Journal of Mechanical Engineering 49 (2013) 8-16.

[25]Huang NE, Shen SSP. Hilbert-Huang transform and its applications. New Jersey: World Scientific Publishing Co. Pte. Ltd. 2005.

[26]Jin XS, Wu Y, Liang SL, Wen ZF. Mechanisms and countermeasures of out-of-roundness wear on railway vehicle wheels. Journal of Southwest Jiaotong University 53(1) (2018) 1-14.

[27]Zhou L, Ding HH, Han ZY, Chen CM, Liu QY, Guo J, Wang WJ. Study of rolling-sliding contact damage and tribo-chemical behaviour of wheel-rail materials at low temperatures. Engineering Failure Analysis 134 (2022) 106077.

[28]Pan R, Ren RM, Chen CH, Zhao XJ. Formation of nanocrystalline structure in pearlitic steels by dry sliding wear. Wear 132 (2017) 397-404.

[29]Snyder T, Stone DH, Kristan J. Wheel flat and out-of round formation and growth. Proceedings of the 2003 IEEE/ASME Joint Railroad Conference (2003) 143-148.

[30]Morys B. Enlargement of out-of-round wheel profiles on high speed trains. Journal of Sound and Vibration 227(5) (1999) 965-978.

[31]Luo R, Zeng J, Wu PB, Dai HY. Simulation and analysis of wheel out-of-roundness wear of high-speed train. Journal of the China Railway Society 32(5) (2010) 30-35.

[32]Qu S, Zhu B, Zeng J, Dai HY, Wu PB. Experimental investigation for wheel polygonisation of high-speed trains. Vehicle System Dynamics 59(10) (2020) 1573-1586.

[33]Dekker H. Vibrational resonances of nonrigid vehicles: Polygonization and ripple patterns. Applied Mathematical Modelling 33(3) (2009) 1349-1355.

[34]Hu Y, Watson M, Maiorino M, Zhou L, Wang WJ, Ding HH, Lewis R, Meli E, Rindi A, Liu QY, Guo J. Experimental study on wear properties of wheel and rail materials with different hardness values. Wear 477 (2021) 203831.

[35]Zeng DF, Lu LT, Zhang YB, Zhang JW, Wen ZF, Zhu MH. Effect of alloy content on rolling contact wear of high-speed wheel material. Tribology 32(6) (2012) 599-605.